

Electron solvation in water clusters following charge transfer from iodide

Jan R. R. Verlet, Aster Kammrath, Graham B. Griffin, and Daniel M. Neumark^{a)}

Department of Chemistry, University of California, Berkeley, California 94720

and Chemical Science Division, Lawrence Berkeley National Laboratory, Berkeley, California 94720

(Received 20 September 2005; accepted 21 October 2005; published online 16 December 2005)

The dynamics following charge transfer to solvent from iodide to a water cluster are studied using time-resolved photoelectron imaging of $\text{I}^-(\text{H}_2\text{O})_n$ and $\text{I}^-(\text{D}_2\text{O})_n$ clusters with $n \leq 28$. The results show spontaneous conversion, on a time scale of ~ 1 ps, from water cluster anions with surface-bound electrons to structures in which the excess electron is more strongly bound and possibly more internalized within the solvent network. The resulting dynamics provide valuable insight into the electron solvation dynamics in water clusters and the relative stabilities between recently observed isomers of water cluster anions. © 2005 American Institute of Physics.

[DOI: 10.1063/1.2137314]

The hydrated electron is a ubiquitous species in aqueous solution and has important implications for various processes such as charge transfer, chemical reactivity, and radiation chemistry. It is generally believed to be localized within a roughly spherical cavity formed by a number of water molecules^{1,2} and has been extensively studied since its discovery.³ This body of work has motivated numerous studies of water cluster anions $(\text{H}_2\text{O})_n^-$, with the goal of obtaining additional insight into the electron-water interaction that governs the properties of the bulk hydrated electron.⁴⁻¹³ For example, time-resolved studies in the cluster anions^{10,11} have yielded new insights into the electronic relaxation dynamics of the hydrated electron, while infrared spectroscopy⁹ has revealed novel electron-water binding motifs in the clusters. In this contribution, we apply time-resolved photoelectron imaging¹⁴ to large $\text{I}^-(\text{H}_2\text{O})_n$ clusters in order to gain further insight into the electron-water interactions that govern the spectroscopy and dynamics in the clusters and the bulk. The experiments show that introduction of the excess electron originally on the iodide anion into the solvent network results in isomerization to a structure in which this electron is more strongly bound.

The work reported here was motivated by recent photoelectron (PE) spectra¹² on water cluster anions $(\text{H}_2\text{O})_n^-$, $11 \leq n \leq 150$, that showed evidence for multiple isomers over a broad range of cluster sizes. In addition to the isomer previously seen in the PE spectra of Coe *et al.*,⁶ we observed a new class of $(\text{H}_2\text{O})_n^-$ clusters with significantly lower vertical binding energy (VBE), the energy required to remove the electron from the anion without nuclear rearrangement. The clusters with higher and lower VBEs were labeled isomers I and II, respectively. Molecular dynamics simulations predict that clusters with surface-bound states have lower VBEs than those with internalized electrons.^{5,13} This led us to assign I and II to clusters with internalized and surface-bound electrons, respectively, although the assignment of isomer I has

recently been called into question.¹³ The lower VBEs for isomer II suggested that it was a higher-energy form of the anion than isomer I. However, it was preferentially generated under conditions normally associated with the production of cold clusters; this observation was taken to indicate that the isomer II clusters were metastable species trapped in a potential energy local minimum.

One of the more intriguing results from the simulations of Barnett *et al.*^{15,16} was the prediction that the surface states of large water cluster anions spontaneously isomerize to internal states on a time scale of about 1 ps. This result provides further motivation for the work reported here, in which we explore the dynamics of isomerization between isomers II and I. Initial efforts to observe isomerization via photoexcitation of isomer II clusters were not successful,¹⁷ and here we apply a different approach based on time-resolved PE imaging of $\text{I}^-(\text{H}_2\text{O})_n$ clusters. This approach enables us to introduce an electron onto the surface of a neutral water cluster, and observe the ensuing dynamics.

The idea stems from a common and elegant means of generating hydrated electrons in liquid water,¹⁸ which uses a solute ion, typically iodide, to inject an electron into the water through the so-called charge-transfer-to-solvent (CTTS) states.¹⁹ Such transitions have also been observed in small clusters of $\text{I}^-(\text{H}_2\text{O})_n$ (Ref. 20) and appear to converge to the bulk absorption band. The critical aspect of $\text{I}^-(\text{H}_2\text{O})_n$ clusters for the present study is that the I^- resides on the surface of the water cluster for sizes $n \leq 28$.^{21,22} Excitation of the CTTS band may consequently be expected to transfer the electron from the iodide to the surface of the water cluster, forming $\text{I} \cdots (\text{H}_2\text{O})_n^-$, the evolution of which is then monitored with time.

The femtosecond pump-probe experiment has been outlined in detail elsewhere^{23,24} and is similar to the previous studies on $\text{I}^-(\text{H}_2\text{O})_n$.^{25,26} These, however, focused on small clusters, with $n < 11$, since the pump photon energy, 4.7 eV, was insufficient to access the CTTS state for larger clusters. These smaller clusters exhibited dynamics assigned to solvation of the excess electron, but were too small to support internalized electrons.^{9,27}

^{a)} Author to whom correspondence should be addressed. Electronic mail: dneumark@berkeley.edu

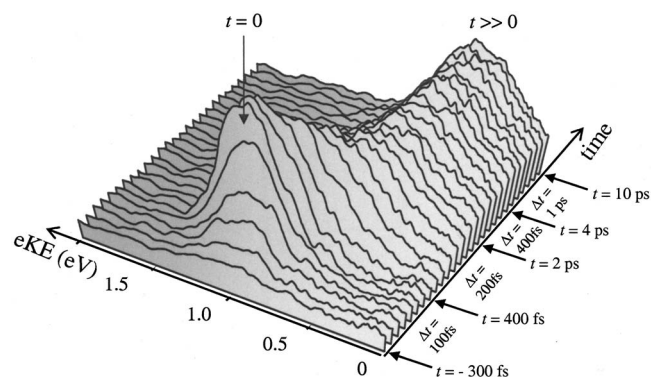


FIG. 1. Time-resolved photoelectron spectra for $\text{I}\cdots(\text{D}_2\text{O})_{17}^-$ following charge transfer from the iodide to the water cluster in $\Gamma(\text{D}_2\text{O})_{17}$. Time steps are indicated on the time axis.

Here, use of a higher pump photon energy enables us to investigate larger clusters with $11 \leq n \leq 28$. We produce $\Gamma(\text{H}_2\text{O})_n$ or $\Gamma(\text{D}_2\text{O})_n$ clusters in an electron-rich molecular-beam expansion and inject them into a time-of-flight mass spectrometer. Mass-selected clusters interact with pump and probe laser pulses. Resulting photoelectrons are mapped²⁸ onto a position-sensitive detector yielding photoelectron images, which are acquired at various pump-probe delays. PE spectra are extracted from the images using standard methods.²⁹ Pump and probe pulses are derived from a commercial regenerative amplified Ti:sapphire laser delivering 80 fs pulses at 800 nm. Pump pulses are generated by sum-frequency mixing of the fundamental with the signal output from an optical parametric amplifier at 1200 nm. The resulting light is then frequency doubled, yielding $\sim 2 \mu\text{J}/\text{pulse}$ at 242 nm. The 800 nm fundamental is used to probe the dynamics by photodetaching the electron, and the experimental resolution is < 200 fs. The 242 nm pump, corresponding to 5.1 eV, is close to the bulk CTTS absorption maximum at 5.5 eV.¹⁹

Figure 1 shows a plot of the temporally evolving PE kinetic energy [$eKE(t)$] with increasing pump-probe delay for $\Gamma(\text{D}_2\text{O})_{17}$. The PE signal begins to grow in as the pump precedes the probe and is centered at $eKE(t \sim 0) = 1.05$ eV. The PE peak then shifts towards lower eKE , corresponding to higher VBE, ultimately converging to $eKE(t \gg 0) = 0.51$ eV. This shift occurs on a time scale of 850 fs.

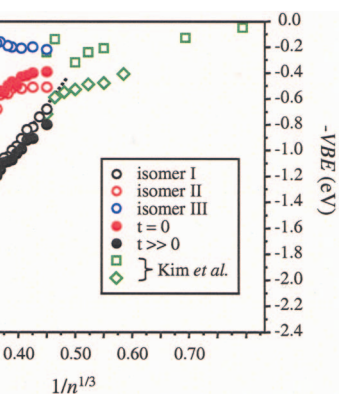
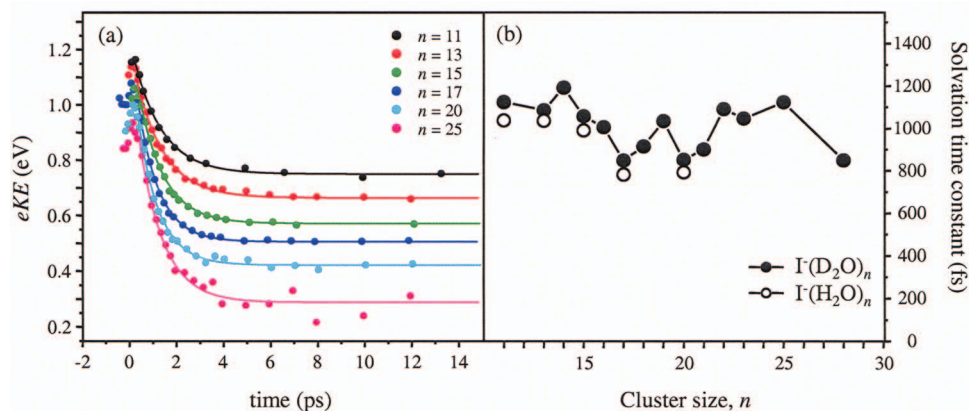


FIG. 3. (Color) Comparison between the photoelectron spectra, plotted in terms of electron binding energy ($eBE = h\nu - eKE$), taken for $\text{I}\cdots(\text{D}_2\text{O})_{20}$ at times $t \sim 0$ ps (a) and $t = 12$ ps (b) and that taken for $(\text{D}_2\text{O})_{20}^-$ under conditions where the additional isomers could be observed (blue line) (Ref. 12). The vertical dashed line indicates the vertical binding energies (VBE) of isomer II and isomer I in (a) and (b), respectively. (c) Shows a comparison between the VBEs measured around zero pump-probe delay and at long (12 ps) delay, and the VBEs reported for various isomers of $(\text{H}_2\text{O})_n^-$ (Ref. 12). The symbols are shown in the legend, where the data for small clusters are taken from Ref. 8.

Similar trends are observed for all clusters studied with $n = 11 - 28$. The time-dependent electron kinetic energy at which the PE signal is maximal, $eKE_{\text{max}}(t)$, may be related to instantaneous vertical binding energy $\text{VBE}(t)$ of the cluster by $\text{VBE} = h\nu - eKE_{\text{max}}$. Time-dependent VBEs are graphed for selected $\text{I}\cdots(\text{D}_2\text{O})_n^-$ clusters in Fig. 2(a), where $\text{VBE}(t)$ has been determined for each time delay by fitting the photoelectron peak to a Gaussian function. The $\text{VBE}(t)$ fit single exponential decays, which are overlaid onto the experimental data in Fig. 2(a). These fits yield time constants that vary nonmonotonically between $\tau = 850$ and 1200 fs for $\text{I}\cdots(\text{D}_2\text{O})_n^-$. The $\text{I}\cdots(\text{H}_2\text{O})_n^-$ isotopomers generally exhibit slightly faster decays, but any differences are comparable to the uncertainty in determining the time scales, which is on the order of ± 50 fs for $n < 20$ and ± 100 fs for larger clusters. All time scales for the clusters studied are shown in Fig. 2(b). In addition to the dynamics in Fig. 2(a), autodetachment is observed for clusters with $n < 15$, yielding very low-energy electrons.²⁶ This process occurs on a time scale of several nanoseconds and therefore has no bearing on the results discussed here.

Figures 3(a) and 3(b) compare the PE spectrum of

FIG. 2. (Color) (a) Dynamics of the measured electron kinetic energy (eKE) with pump-probe delay for a range of $\text{I}\cdots(\text{D}_2\text{O})_n^-$ clusters. Data points are indicated as such in the legend and single exponential decay fits are shown as solid lines. (b) Time constants taken from single exponential fits [see (a)] to the shift in eKE for both $\text{I}\cdots(\text{D}_2\text{O})_n^-$ (full circles) and $\text{I}\cdots(\text{H}_2\text{O})_n^-$ (open circles).

$(D_2O)_{20}^-$ (blue line) to the time-dependent PE spectra of $I \cdots (D_2O)_{20}^-$ for $t \sim 0$ (a) and $t = 12$ ps (b). The PE spectrum of $(D_2O)_{20}^-$ was taken under conditions where both isomers may be identified; isomer I is the main peak, while isomer II is the smaller feature at lower binding energy, whose VBE is indicated by the dashed line in Fig. 3(a). The VBE for $I \cdots (D_2O)_{20}^-$ at $t \sim 0$ is very close to that for isomer II. At $t = 12$ ps, the entire time-dependent PE spectrum is in excellent agreement with that of isomer I. In Fig. 3(c), the VBEs for these two limiting cases are plotted along with the VBEs reported for $(H_2O)_n^-$ and $(D_2O)_n^-$ clusters under varying source conditions.¹² These show the existence of the three isomers, labeled I, II, and III for sizes $n \geq 11$. For smaller clusters, a number of isomers have also been reported.⁸ The correlation between VBE ($t \sim 0$) and the VBE of isomer II, and between VBE ($t = 12$ ps) and the VBE of isomer I is striking, and agreement between the two sets of values improves with increasing cluster size.

The data plotted in Figs. 2 and 3 reveal several fundamental aspects of $I^-(H_2O)_n$ and $(H_2O)_n^-$ clusters. The VBE shifts in Fig. 2(a) show that the excess electron becomes more strongly bound to the cluster over time. There has been some discussion in the literature regarding whether these shifts originate from stabilization of the excess electron in $I^-(H_2O)_n$ clusters via solvent motion, as was originally proposed by us,²⁵ or if instead they result from the I atom leaving the cluster.³⁰ For the much smaller clusters initially studied ($n=4-6$), the magnitudes of the shifts were sufficiently small (0.1–0.3 eV) that it was difficult to distinguish between the two mechanisms. However, Fig. 3(c) shows that the shift becomes progressively larger with increasing n , and reaches 0.7 eV by $n=25$. Both the size-dependent trend and magnitude of the shift strongly toward solvent stabilization as the primary mechanism here. The slightly higher VBE ($t=12$ ps) values compared to the isomer I clusters may reflect a residual effect of the I atom, consistent with recent experiments on smaller $I^-(H_2O)_n$ clusters suggesting that I atom loss, signified by a small shift in VBE, does not occur until ~ 50 ps.²⁶

Comparison of the VBEs in Fig. 3 indicates very close correspondences between $I^-(H_2O)_n$ just after CTTS excitation and isomer II of the $(H_2O)_n^-$ cluster of the same size, and between $I^-(H_2O)_n$ at longer times and isomer I of $(H_2O)_n^-$. Hence, we are apparently observing spontaneous conversion, on a time scale of ~ 1 ps, from isomer II, with the excess electron initially at the surface of the cluster, to isomer I. The iodine atom appears to be a spectator in this process, at least from an energetic point of view. This spontaneous isomerization process indicates that isomer I has a lower energy (or, more precisely, free energy) than isomer II. While one might assume isomer I clusters to be lower in energy because of their higher VBEs, this assumption fails when different structural isomers are involved,³¹ since the VBEs reflect energy differences between anion and neutral isomers of the same geometry.

In our earlier work on pure water cluster anions,¹² we proposed that the isomer II clusters formed under “cold” ion source conditions were higher energy, metastable species, that were trapped in a local potential-energy minimum. In

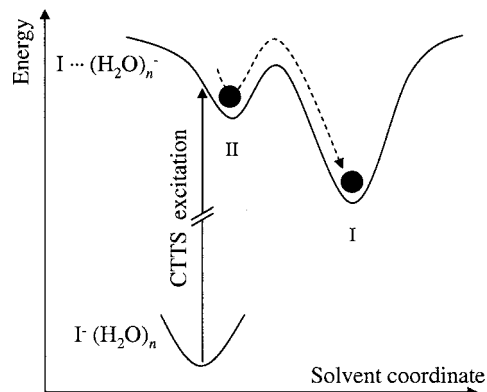


FIG. 4. Representative energy diagram showing schematically the dynamics observed. Upon CTTS excitation, the $I \cdots (H_2O)_n^-$ cluster resembles isomer II of the bare $(H_2O)_n^-$ cluster. The cluster then undergoes spontaneous isomerization to form a cluster characteristic of isomer I.

fact, for all clusters studied here except the largest ($n \leq 25$), isomer II clusters were only observed for $(D_2O)_n^-$ clusters, a result attributed to higher zero-point energy and more facile tunneling in $(H_2O)_n^-$ clusters that would make them harder to contain in a shallow potential-energy well. The results found here support our proposed energy ordering. One can also understand why spontaneous isomerization occurs for the electronically excited $I \cdots (D_2O)_n^-$ clusters reported here but not for bare $(D_2O)_n^-$ isomer II clusters in our earlier work; the halide-water clusters are likely to be considerably warmer than the pure water cluster anions were under conditions that produced isomer II clusters. A representative energy diagram showing schematically the dynamics observed here is presented in Fig. 4.

The nature of the solvent coordinate in Fig. 4 is of considerable interest. The molecular-dynamics simulations of Barnett *et al.*^{15,16} investigated solvation of a diffuse excess electron initially on the surface of an equilibrated neutral $(H_2O)_{256}$ cluster at 300 K. The electron was found to localize on the surface of the cluster within 150 fs, then evolved by sampling a number of binding sites before penetrating the surface, 1.2 ps after initial attachment, and becoming fully internally solvated on a 1 ps time scale. Although the cluster size in the simulations is considerably larger, qualitative agreement with the calculated energetics is notable. Additionally, the calculated time scale for the actual internalization process is in remarkable agreement to the isomerization time scale observed in our experiments.

These considerations, along with the correspondences between our time-dependent VBEs and those for isomers I and II of the bare water cluster anions, raise the intriguing possibility that we are observing isomerization of the excess electron from a surface to an internalized state. However, recent theoretical and experimental^{13,27} works have raised the question as to whether isomer I is an internalized state, or is instead another surface-bound state with a different (and stronger) electron binding motif. Thus, a definitive interpretation of the solvent coordinate in Fig. 4 awaits a fuller understanding of the isomer I clusters.

This work is supported by the National Science Foundation under Grant No. CHE-0350585. The authors thank Professor Ori Cheshnovsky for many interesting discussions.

- ¹L. Kevan, *Acc. Chem. Res.* **14**, 138 (1981).
- ²P. J. Rossky and J. Schnitker, *J. Phys. Chem.* **92**, 4277 (1988).
- ³E. J. Hart and J. W. Boag, *J. Am. Chem. Soc.* **84**, 4090 (1962).
- ⁴U. Landman, R. N. Barnett, C. L. Cleveland, D. Scharf, and J. Jortner, *J. Phys. Chem.* **91**, 4890 (1987).
- ⁵R. N. Barnett, U. Landman, C. L. Cleveland, and J. Jortner, *J. Chem. Phys.* **88**, 4429 (1988).
- ⁶J. V. Coe, G. H. Lee, J. G. Eaton, S. T. Arnold, H. W. Sarkas, K. H. Bowen, C. Ludewight, H. Haberland, and D. R. Worsnop, *J. Chem. Phys.* **92**, 3980 (1990).
- ⁷P. Ayotte and M. A. Johnson, *J. Chem. Phys.* **106**, 811 (1997).
- ⁸J. Kim, I. Becker, O. Cheshnovsky, and M. A. Johnson, *Chem. Phys. Lett.* **297**, 90 (1998).
- ⁹N. I. Hammer, J. W. Shin, J. M. Headrick, E. G. Diken, J. R. Roscioli, G. H. Weddle, and M. A. Johnson, *Science* **306**, 675 (2004).
- ¹⁰A. E. Bragg, J. R. R. Verlet, A. Kammrath, O. Cheshnovsky, and D. M. Neumark, *Science* **306**, 669 (2004).
- ¹¹D. H. Paik, I. R. Lee, D. S. Yang, J. S. Baskin, and A. H. Zewail, *Science* **306**, 672 (2004).
- ¹²J. R. R. Verlet, A. E. Bragg, A. Kammrath, O. Cheshnovsky, and D. M. Neumark, *Science* **307**, 93 (2005).
- ¹³L. Turi, W. S. Sheu, and P. J. Rossky, *Science* **309**, 914 (2005).
- ¹⁴A. Stolow, A. E. Bragg, and D. M. Neumark, *Chem. Rev. (Washington, D.C.)* **104**, 1719 (2004).
- ¹⁵R. N. Barnett, U. Landman, and A. Nitzan, *J. Chem. Phys.* **91**, 5567 (1989).
- ¹⁶R. N. Barnett, U. Landman, and A. Nitzan, *Phys. Rev. Lett.* **62**, 106 (1989).
- ¹⁷A. E. Bragg, J. R. R. Verlet, A. Kammrath, O. Cheshnovsky, and D. M. Neumark, *J. Am. Chem. Soc.* **127**, 15283 (2005).
- ¹⁸J. Jortner, M. Ottolenghi, and G. Stein, *J. Phys. Chem.* **68**, 247 (1964).
- ¹⁹M. F. Fox and E. Hayon, *J. Chem. Soc., Faraday Trans. 1* **73**, 1003 (1977).
- ²⁰D. Serxner, C. E. H. Dessent, and M. A. Johnson, *J. Chem. Phys.* **105**, 7231 (1996).
- ²¹O. Cheshnovsky, R. Giniger, G. Markovich, G. Makov, A. Nitzan, and J. Jortner, *J. Chim. Phys. Phys.-Chim. Biol.* **92**, 397 (1995).
- ²²D. M. Koch and G. H. Peslherbe, *Chem. Phys. Lett.* **359**, 381 (2002).
- ²³A. E. Bragg, J. R. R. Verlet, A. Kammrath, and D. M. Neumark, *J. Chem. Phys.* **121**, 3515 (2004).
- ²⁴A. V. Davis, R. Wester, A. E. Bragg, and D. M. Neumark, *J. Chem. Phys.* **118**, 999 (2003).
- ²⁵L. Lehr, M. T. Zanni, C. Frischkorn, R. Weinkauff, and D. M. Neumark, *Science* **284**, 635 (1999).
- ²⁶A. Kammrath, J. R. R. Verlet, A. E. Bragg, G. B. Griffin, O. Cheshnovsky, and D. M. Neumark, *J. Phys. Chem. A* (in press).
- ²⁷N. I. Hammer, J. R. Roscioli, and M. A. Johnson, *J. Phys. Chem. A* **109**, 7896 (2005).
- ²⁸A. Eppink and D. H. Parker, *Rev. Sci. Instrum.* **68**, 3477 (1997).
- ²⁹V. Dribinski, A. Ossadtchi, V. A. Mandelshtam, and H. Reisler, *Rev. Sci. Instrum.* **73**, 2634 (2002).
- ³⁰H. Y. Chen and W. S. Sheu, *Chem. Phys. Lett.* **335**, 475 (2001).
- ³¹A. Martinez, L. E. Sansores, R. Salcedo, F. J. Tenorio, and J. V. Ortiz, *J. Phys. Chem. A* **106**, 10630 (2002).